

Compressive pseudoelastic behavior in copper nanowires

Sangjin Lee,¹ Byeongyong Lee,² and Maenghyo Cho^{1,*}¹WCU Multiscale Mechanical Design Division, School of Mechanical and Aerospace Engineering, Seoul National University, Seoul 151-742, Korea²Stainless Steel Research Group, Posco, Pohang, Gyeongbuk 790-300, Korea

(Received 24 July 2009; revised manuscript received 23 April 2010; published 8 June 2010)

We predict the pseudoelasticity of the $\langle 100 \rangle / \{100\}$ copper nanowire using atomistic simulations with the embedded atom method potential under uniaxial compressive loading. The $\langle 100 \rangle / \{100\}$ copper nanowire exhibits pseudoelasticity which depends on the reorientation of the crystalline structure of the nanowire due to twinning. The twinning that governs the pseudoelasticity of the $\langle 100 \rangle / \{100\}$ nanowire results from an external compressive loading whereas the twinning that governs the pseudoelasticity of the $\langle 110 \rangle / \{111\}$ nanowire results from a tensile loading. Therefore, the pseudoelasticity of the $\langle 100 \rangle / \{100\}$ nanowire is referred to as “compressive pseudoelasticity.” This difference in the twinning phenomena distinguishes the $\langle 100 \rangle / \{100\}$ nanowire from the $\langle 110 \rangle / \{111\}$ nanowire. This study also shows that the pseudoelasticity of the nanowire is related to the stacking-fault energy of the nanowire material and the Schmid factor which depends on the structural orientation of the nanowire. The $\langle 100 \rangle / \{100\}$ nanowire shows the maximum recoverable strain of 22% which is a remarkable amount compared with 5–10 % for bulk shape memory alloys. In addition, the $\langle 100 \rangle / \{100\}$ nanowire does not need to reach the critical temperature to exhibit pseudoelasticity because the lateral free surfaces of the twin region have lower energy than the surface of the nanowire.

DOI: 10.1103/PhysRevB.81.224103

PACS number(s): 61.46.−w, 62.25.−g, 64.70.Nd

I. INTRODUCTION

Recent advances in nanotechnology have facilitated the development of nanoscale materials, such as nanowires, nanotubes, and nanothin films, which have unique characteristics and potential for wide-ranging applications. Among these commonly observed unique characteristics, properties such as high surface-to-volume ratio at the nanometer scale are closely related to the length scale of material. Thus, “surface effect” or “size effect” is often used to describe such key features of nanomaterials. The structural transitions of bulk transition metals induced by a tension or a compression were reported in theoretical studies. A body-centered-cubic crystal structure can be transformed to a face-centered-cubic (fcc) structure under $[100]$ uniaxial tension¹ and can be transformed to a hexagonal-closed-packed structure under $[100]$ uniaxial compression.²

Phase transformation and related mechanical attributes of nanowires have enabled a wide range of applications in the areas of nanoelectromechanical systems (NEMS), actuators, and sensors. Pseudoelasticity of an fcc nanowire is one distinct feature that appears in the nanoscale. In the macro scale, pseudoelasticity, as well as shape memory effect (SME), occurs in very few alloys. However, in the nanoscale, pure fcc metal nanowires exhibit both pseudoelasticity and SME.^{3–7} In the case of bulk shape memory alloys (SMAs), practical applications are limited because of long response times. On the other hand, nanowires have very short response times, on the order of nanoseconds.³ Moreover, the predicted recoverable strains of nanowires are much larger than that of bulk SMAs.^{5,7}

The atomic structure of $\langle 110 \rangle / \{111\}$ fcc nanowires has been considered as the typical structure for studying pseudoelasticity of nanowires, in previous studies.^{6,7} Pseudoelasticity is an inelastic behavior related to the deformation

mechanism, twinning, which is affected by important parameters⁸ including the structural orientation of the nanowire, the loading condition, and the transverse free-surface orientation of the nanowire. In the case of $\langle 110 \rangle / \{111\}$ fcc nanowires, not only should the mechanical loading be controlled but also should the critical temperature of the phase transformation, to ultimately control pseudoelasticity.

In this study, the pseudoelasticity of $\langle 100 \rangle / \{100\}$ fcc nanowires, which can be made using a top-down fabrication process,^{9–12} is investigated. Using molecular dynamics (MD) simulations, it is shown that the $\langle 100 \rangle / \{100\}$ fcc nanowire exhibits pseudoelasticity under reorientation conditions, different from those of the $\langle 110 \rangle / \{111\}$ fcc nanowire. The pseudoelasticity of $\langle 100 \rangle / \{100\}$ nanowire is different from that of the $\langle 110 \rangle / \{111\}$ nanowire mainly because of the loading condition, reorientation process, and the temperature condition for pseudoelasticity.

II. MATERIALS AND METHODS

In this study, MD simulations are used to investigate the mechanical behavior of nanowires, using the interatomic potential for copper within the embedded atom method (EAM) by Mishin *et al.*¹³ The EAM assumes that the total energy of metals consists of the embedding energy term and the pair interaction term, as below,¹⁴

$$E_{tot} = \sum_i F_i(\rho_{h,i}) + \frac{1}{2} \sum_{i,j} \phi_{ij}(R_{ij}), \quad (1)$$

$i \neq j$

where ϕ_{ij} is the pair potential and R_{ij} is the distance between the pair of atoms i and j . $\rho_{h,j}$ is the total host electron density at atom j , which is a function of R_{ij} , and F_i is the embedding energy. By incorporating the embedding energy term, which

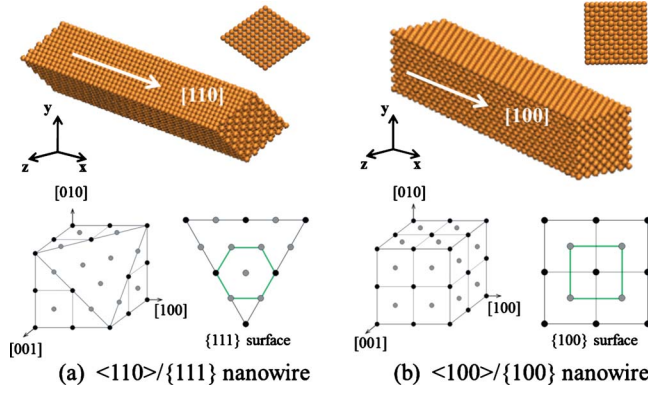


FIG. 1. (Color online) (a) Snapshot of $\langle 110 \rangle / \{111\}$ fcc copper nanowire with $\langle 110 \rangle$ longitudinal axis and $\{111\}$ transverse surfaces, and a schematic drawing of the $\{111\}$ surface; (b) a $\langle 100 \rangle / \{100\}$ fcc copper nanowire with $\langle 100 \rangle$ longitudinal axis and $\{100\}$ transverse surfaces, and a schematic drawing of the $\{100\}$ surface. Graphics are generated by VMD 1.8.6 (Ref. 20).

is an approximation of many-body interactions, the EAM simplifies the total-energy calculation for metallic systems and reduces the complexity of a system to a practical level for computation.¹⁵ On the other hand, first-principles calculations are impractical in resolving complex systems, such as interfaces, surfaces, and grain boundaries because they involve solving the many-electron Schrödinger equation.¹⁵

In the description of plastic deformation of fcc transient metals, the accuracy of the stacking-fault energy (SFE) is most important because it is the parameter closely related to the nucleation and propagation of the dislocation.^{5,16–18} The SFE of the EAM, developed by Mishin *et al.*, is in good agreement^{5,13} with the experimental results (intrinsic/stable stacking-fault energy) and the first-principles calculation results (generalized stacking-fault energy curves). Thus, this EAM gives a more accurate description of the copper atoms than other EAM potentials.^{14,19} For these reasons, the EAM developed by Mishin *et al.* is chosen to study the mechanical behavior of copper nanowires.

The $\langle 110 \rangle / \{111\}$ nanowire, studied by previous researchers, has four $\{111\}$ transverse surfaces and a rhombic cross section with the longitudinal direction along $\langle 110 \rangle$,^{6,7} as shown in Fig. 1(a). The $\{111\}$ surface can be easily represented by a hexagonal honeycomb.^{3–6} In this study, $\langle 100 \rangle / \{100\}$ copper nanowires, which have a single-crystalline fcc structure, are considered. The $\langle 100 \rangle / \{100\}$ nanowire has four $\{100\}$ transverse free surfaces with $\langle 100 \rangle$ directional longitudinal axis, as shown in Fig. 1(b). The size of the $\langle 100 \rangle / \{100\}$ nanowire is 10.84 nm (30 lattice constant units) along the longitudinal direction and has a $2.16 \times 2.16 \text{ nm}^2$ (six lattice constant units) cross section. The lattice constant of the nanowire is determined from that of an equilibrated bulk single-crystalline structure of 0.3615 nm. However, the lattice constant is not an energetically stable value in the nanoscale because a large surface stress for the reduction in the surface energy is induced by the high surface-to-volume ratio. Thus, a relaxation process is needed to equilibrate the $\langle 100 \rangle / \{100\}$ nanowire. During relaxation, the nanowire is equilibrated at constant temperature, which

corresponds to simulating for 5 ns under the free boundary condition. The Nosé-Hoover NVT ensemble simulation²¹ is used to maintain the isothermal condition.

After the relaxation process, both ends of the nanowire are fixed. Then, a strain load is applied on one end of the nanowire, along the longitudinal direction, by moving the constrained atoms repeatedly, followed by the relaxation process using the NVT ensemble condition. The direction of the external strain load decides whether the nanowire is unidirectionally stretched or compressed. The displacement of the constrained atoms at each loading step is 2.5% of the unit lattice length of copper (9.0375 pm). Once each strain load is applied at the fixed atoms, the nanowire is equilibrated for 200 ps, with both ends fixed.

The cyclic loading condition applied on the $\langle 100 \rangle / \{100\}$ nanowire is as follows: (1) the nanowire is compressed until inelastic deformation occurs on the nanowire; (2) after the nanowire experiences inelastic deformation under compression, the constrained end of the nanowire moves in the reversed direction (tensile direction) until the stress reaches the zero stress state; (3) the constrained atoms are made to move in the same direction, resulting in the extension state; and (4) the constrained atoms are moved in the reversed direction (compressive direction) until the stress reaches the initial zero stress state.

In this study, the periodic boundary condition is not used, and all simulations are performed using the Sandia National Laboratories developed code, LAMMPS.²²

III. SIMULATION RESULTS

A. Pseudoelasticity at 300 K

1. Pseudoelasticity of nanowire and the reversibility of twinning

The stress-strain curve of a copper nanowire at 300 K, during the first cyclic loading, and the snapshots of the nanowire, are shown in Fig. 2. The $\langle 100 \rangle / \{100\}$ copper nanowire exhibits pseudoelastic behavior under cyclic loading, which consists of four steps—compressive loading, unloading, tensile loading, and unloading. The nanowire deforms during the cyclic loading and recovers to the initial undeformed state in the end.

The nanowire, at the initial state, has a perfect crystalline structure, without any defects, as shown at point A in Figs. 2(b) and 2(c). During compressive loading [the A-C section in Fig. 2(a)], the nanowire undergoes inelastic deformation governed by twinning, as depicted in B and C of Figs. 2(b) and 2(c). In other words, as the compressive load increases, yielding occurs by twinning and the twin boundary propagates with the dilation of twinning or multiple twins appear. Once the compressive loading ends, the nanowire undergoes unloading. During subsequent tensile loading, the deformed region of the nanowire decreases as if twinning unfolds [D and E in Figs. 2(b) and 2(c)]. After an adequate tensile load is applied, the nanowire recovers its original orientation without twinning, which occurs at point F in Figs. 2(b) and 2(c). Finally, during the unloading process [the F-A section in Fig. 2(a)], the pseudoelastic behavior of the nanowire comes to an end. The stress-strain curve completes the hys-

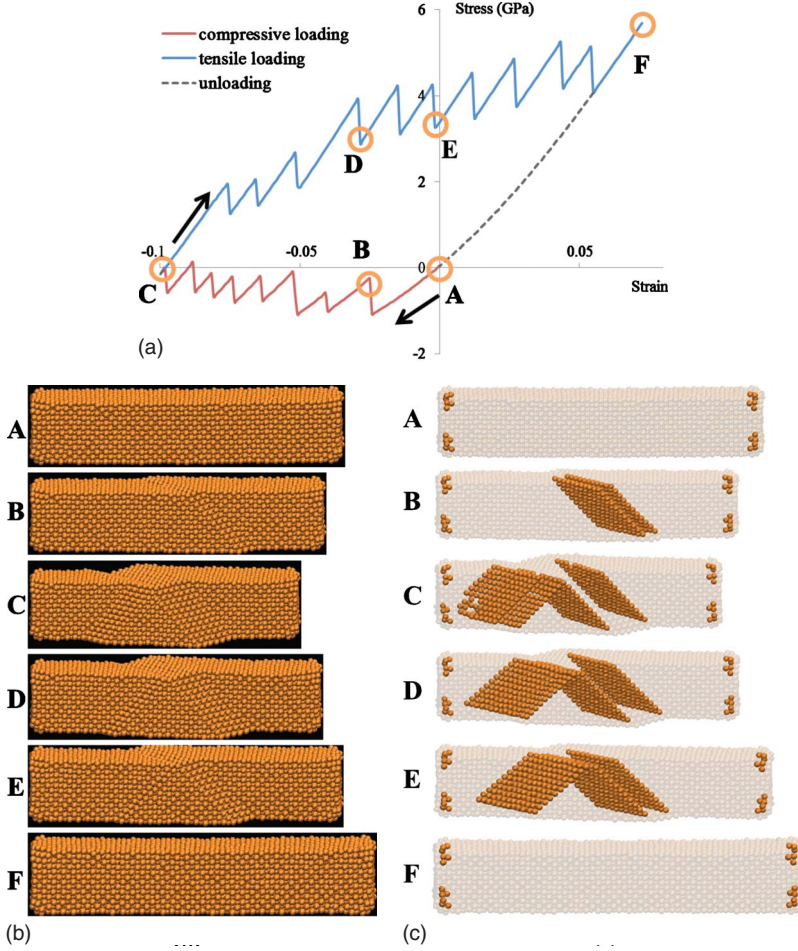


FIG. 2. (Color online) (a) The stress-strain curve of the $\langle 100 \rangle / \{100\}$ Cu nanowire under cyclic loading at 300 K; (b) snapshots of the nanowire corresponding to selected points on the stress-strain curve; and (c) changes in the twin region in the nanowire; the planes on the twin boundary are highlighted by the centrosymmetry parameter (Ref. 28).

teresis loop consisting of the above four steps during the cyclic loading.

Twinning, one of the inelastic deformation mechanisms, appears on the $\langle 100 \rangle / \{100\}$ Cu nanowire during compressive loading, and disappears during the subsequent tensile loading. This reversibility of twinning, depending on the loading condition, is a key factor in the pseudoelasticity of nanowires. Thus, it is important to understand this phenomenon to interpret the pseudoelastic mechanism of $\langle 100 \rangle / \{100\}$ nanowires.

With regard to the reversibility of twinning, it must be understood first that twinning is a deformation mechanism⁶ of the $\langle 100 \rangle / \{100\}$ fcc nanowire, under uniaxial compressive loading. Twinning originates from Shockley partial dislocations. The partial dislocations occur along the $\langle 112 \rangle$ direction, on the $\{111\}$ close-packed plane of the fcc structure. The application of the Frank energy criterion²³ shows that the separation of a full dislocation (\mathbf{b}_1) into two partial dislocations ($\mathbf{b}_2 + \mathbf{b}_3$) is more energetically favorable,²⁴

$$\mathbf{b}_1 \rightarrow \mathbf{b}_2 + \mathbf{b}_3,$$

$$\frac{a_0}{2}[10\bar{1}] \rightarrow \frac{a_0}{6}[2\bar{1}\bar{1}] + \frac{a_0}{6}[11\bar{2}], \quad (2)$$

where vector \mathbf{b}_i defines the slip directions, as shown in Fig. 3. The decomposition process reduces the strain energy pro-

portional to the change $(a_0^2)/2 \rightarrow (a_0^2)/3$. The deformation mechanisms of the fcc structure originate from the nucleation and the propagation of partial dislocations. Slip, the other inelastic deformation mechanism, on one hand, is produced by the integration of the nucleations of the leading partial dislocation and the subsequent trailing partial dislocation on the same $\{111\}$ slip plane, such as $\mathbf{b}_2 + \mathbf{b}_3$. On the other hand, twinning is produced by the integration of the nucleations of the leading partial dislocation and subsequent

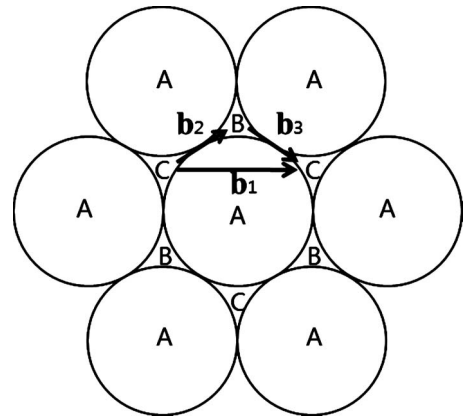


FIG. 3. A schematic drawing of the decomposition of a full dislocation to two partial dislocations on the close-packed $\{111\}$ plane.

TABLE I. Schmid factors for $\langle 100 \rangle$ and $\langle 110 \rangle$ wires, under uniaxial tension and compression (reproduced from Refs. 8 and 26).

Orientation	Schmid factors			
	Tension		Compression	
	Slip	Twinning	Slip	Twinning
$\langle 100 \rangle$	0.42	0.24	0.42	0.47
$\langle 110 \rangle$	0.41	0.48	0.41	0.25

new leading partial (second leading partial) dislocation, such as $\mathbf{b}_2 + \mathbf{b}'_2$. A new leading partial dislocation is nucleated on the other $\{111\}$ slip plane, adjacent to the original $\{111\}$ plane.¹⁷

The major factors that determine whether the deformation mechanism is slip or twinning, are the SFE and the Schmid factor. To generate a partial dislocation, energy is needed to overcome the SFE. The SFE is an energetic barrier to the nucleation and the propagation of a partial dislocation.⁷ Thus SFE, which is considered a material property, influences the determination of the deformation mechanism. Liang and Zhou^{5,6} analyzed twinnability, the parameter that shows the preference of deformation (twinning or slip), based on the dislocation nucleation criterion of Rice¹⁸ and the twinning criterion of Tadmor and Hai.¹⁷ The analysis of twinnability for several metals, including copper, concluded that twinning is favored over slip, and reversible deformation is exhibited through twinning in the case of copper.⁵ However, twinnability cannot explain why the crystalline orientation and the external loading direction provide different results of deformation (twinning or slip) in the same material: $\langle 100 \rangle / \{100\}$ copper nanowire is deformed by slip under tensile loading and by twinning under compressive loading while $\langle 110 \rangle / \{111\}$ copper nanowire is deformed by twinning under tensile loading and by slip under compressive loading. For this reason, the Schmid factor is required because it reflects the crystalline orientation of the material and the external loading direction. Two energy sources are used to overcome the SFE. One is the thermal energy at 300 K (discussed later) and the other is the strain energy caused by the external strain loading. An external axial loading produces not just the energy to overcome the SFE but also the resolved shear stress along the $\{111\}$ slip plane. The resolved shear is related to the Schmid factor, which is the ratio of the resolved shear stress to the axial stress. The Schmid factor purely depends on the geometry of the crystal structure and the external loading direction. The uniaxial Schmid factors for $\langle 100 \rangle$ and $\langle 110 \rangle$ oriented nanowires are shown in Table I. Twinning results in higher Schmid factor than slip, in the case of the $\langle 100 \rangle$ nanowire, under compression. Therefore, twinning occurs more easily than slip in a compressively loaded $\langle 100 \rangle$ nanowire. As mentioned above, the SFE, which is a material property, and the Schmid factor, which is a geometric characteristic, have dominant influences on the determination of the type of deformation mechanism of the nanowire.

The basic physics behind the reversibility of twinning is the reorientation of crystalline structure. Twinning on the $\langle 100 \rangle / \{100\}$ copper nanowire, under compressive loading,

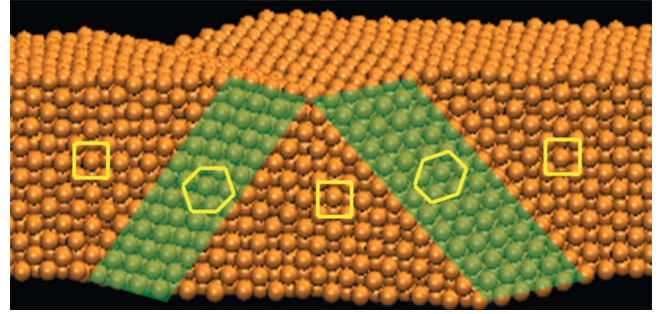


FIG. 4. (Color online) The enlarged snapshot of the nanowire at point C in Fig. 2. The $\langle 100 \rangle / \{100\}$ nanowire has $\{100\}$ transverse surfaces while the deformed region (highlighted with hexagon), by twinning, has $\{111\}$ surfaces which are represented by the honeycomb. This was shown in Fig. 1.

results in the reorientation of the copper nanowire from $\langle 100 \rangle / \{100\}$ to $\langle 110 \rangle / \{111\}$.⁷ In the nanoscale, it induces a reorientation of the nanowire whereas it offers new slip systems by changing the orientation in the continuum level.²⁴ In Fig. 4, the atomic configuration of the $\langle 100 \rangle / \{100\}$ nanowire, deformed due to twinning, is magnified. When twinning appears on the nanowire under compressive loading, twin regions of the nanowire undergo reorientation to $\langle 110 \rangle / \{111\}$. So, the reoriented region of the Cu nanowire has $\{111\}$ side surfaces with a hexagonal array, which have a lower energy compared to $\{100\}$ side surfaces. The $\{111\}$ surface is represented by the honeycomb [in Fig. 1] on a side surface of the twin region, in Fig. 4. The lattice orientation of the twin region and the atomic configuration of the cross sections also reveal the reorientation in the twin region, shown in Fig. 5. The nanowire is aligned along the longitudinal axis $[100]$. As twinning results in the reorientation, the deformed part of nanowire, which is the twin region, has a $[10\bar{1}]$ axis direction and a structure with stacks of close-packed planes (AB-CABC), as shown in Fig. 5(a) and, the cross section in Fig. 5(b) represents the change in the lattice structure. The atomic configuration of the cross section of the deformed part includes twinning in parts. The twin region exhibits a cross-section shape as a rhombus and the $\langle 110 \rangle / \{111\}$ lattice structure while the undeformed nanowire has a square cross section and the $\langle 100 \rangle / \{100\}$ orientation. This reorientation from $\langle 100 \rangle / \{100\}$ to $\langle 110 \rangle / \{111\}$, in the twin region, causes the reversibility of twinning during tensile loading. Basically, as shown in Table I, the deformation mechanism of the $\langle 100 \rangle / \{100\}$ fcc nanowire under tensile loading is slip. However, based on the results discussed above [in Fig. 2], the $\langle 100 \rangle / \{100\}$ nanowire, which has twin regions, does not show slip under tensile loading but reveals the unfolding of the twinning phenomenon. Such behavior is due to the residue of the twinning-induced reorientation in the nanowire. As the twin region has $\langle 110 \rangle / \{111\}$ orientation in the middle of the $\langle 100 \rangle / \{100\}$ nanowire [point C in Figs. 2(b) and 2(c)], the deformation mechanism of the nanowire under tensile loading is not slip but twinning. This precedence of twinning over slip results from the fact that the Schmid factor for the $\langle 110 \rangle$ orientation (0.48) takes priority over that of the $\langle 100 \rangle$ orientation (0.42), under tensile loading, as shown in Table.

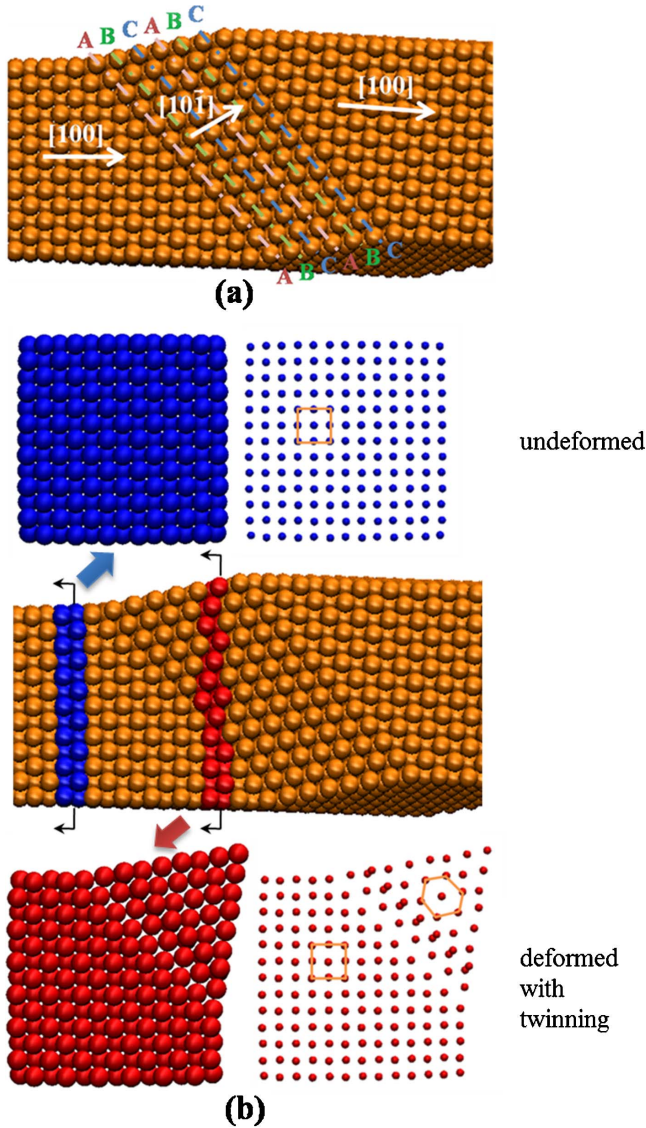


FIG. 5. (Color online) The enlarged snapshot of the twin region in the $\langle 100 \rangle / \{100\}$ nanowire. (a) The lattice orientations in the longitudinal direction are indicated with white arrows. In the twin region, the crystalline structure shows a stacking of close-packed planes. (b) The atomic configurations of the cross sections of the nanowire, including twinning.

I. During tensile loading, (new) twinning appears in the twin region and the $\langle 110 \rangle / \{111\}$ part, and takes precedence over to the slip of $\langle 100 \rangle / \{100\}$ nanowire. This (new) twinning in the twin region induces reorientation from $\langle 110 \rangle / \{111\}$ to $\langle 100 \rangle / \{100\}$, which corresponds to the deformation process of the pseudoelastic behavior of $\langle 110 \rangle / \{111\}$ fcc nanowires.^{3–7,25} Therefore, (new) twinning appears in the twin region under tensile loading, and unfolds the (previous) twinning which was generated under the previous compressive loading [D \rightarrow F in Figs. 2(b) and 2(c)].

In the $\langle 100 \rangle / \{100\}$ copper nanowire, under cyclic loading, twinning, accompanied by reorientation to $\langle 110 \rangle / \{111\}$, appears under compressive loading and generates the twin region; and the subsequent twinning, accompanied by reorientation to $\langle 100 \rangle / \{100\}$, under tensile loading in the twin

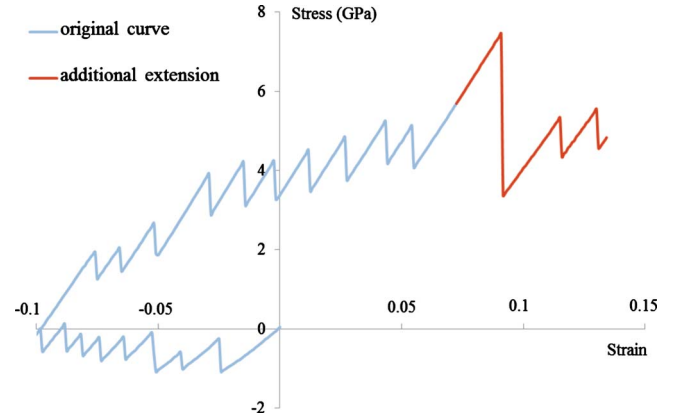


FIG. 6. (Color online) The stress-strain curve of $\langle 100 \rangle / \{100\}$ nanowire, including the additional stretched curve part.

region, removes the twin region. The combination of the compression-induced twinning of the $\langle 100 \rangle / \{100\}$ part and the tension-induced twinning of the $\langle 110 \rangle / \{111\}$ part completes the reversible process of twinning. The reversibility of twinning is the basis of pseudoelasticity of nanowires.

2. Recoverable strain

The nanowire, at point F in Fig. 2, can be stretched by additional tensile loading until yielding occurs due to slip. At the moment when slip appears, the nanowire loses pseudoelasticity because unlike the reversibility of twinning, slip is a permanent plastic deformation; twinning is a reversible deformation mechanism of the $\langle 100 \rangle / \{100\}$ nanowire under compressive loading but slip, which appears on the nanowire under tensile loading, is an irreversible deformation. Thus, the recoverable strain in this case is about 19%, which is the sum of the compression-induced strain (-0.1) and the tension-induced strain (about 0.09 , before slip appears), as shown in Fig. 6. The range of the tension-induced strain is limited by slip and slip occurs at a strain of 0.09 , where the first drop point is in red in Fig. 6. The range of the pseudoelastic behavior of the nanowire exceeds the usual maximum recoverable strain in bulk SMAs (8%).

The maximum recoverable strain of the $\langle 100 \rangle / \{100\}$ Cu nanowire depends on the compression-induced strain because the maximum tension-induced strain is restricted by the slip. The maximum compression-induced strain is about 12%. This value is also determined by the slip action. When a nanowire is deformed by twinning, under compressive loading with a strain of over 12%, slip appears on the nanowire during tensile loading (not always but in many cases). The snapshots of the nanowires that were compressed beyond the critical strain, the maximum compression-induced strain of 12%, show that slips appear on nanowires even after the cyclic loading ended, in Fig. 7. Slip acts like an obstacle to the unfolding of the twinning phenomenon during tensile loading so, the nanowire remains in the deformed state with slip and twinning, even after the cycle has completed. If the nanowire is compressed beyond the maximum allowable strain value, the generation of slip under tensile loading can be explained from a phenomenological point of view. While

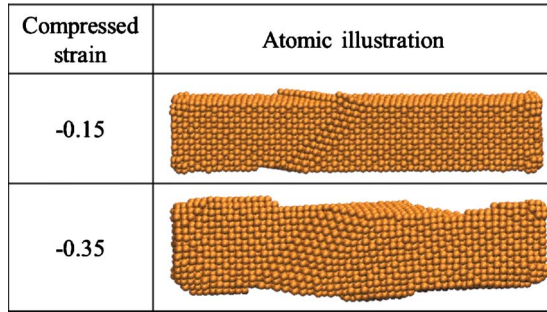


FIG. 7. (Color online) Snapshots of $\langle 100 \rangle / \{100\}$ Cu nanowires under cyclic loading, including the compressive loading over the maximum compression-induced strain value (-0.15 and -0.35 , respectively). Although the tensile loading is applied, nanowires do not recover their initial state because slip occurs.

a nanowire is compressed, each of the twin regions grows [in Fig. 2(b) C]. When the nanowire is compressed beyond the maximum strain value, the twin regions encounter and partly overlap each other. This region, where the twins overlap, can be regarded as the grain boundary. The grain boundary, generated by these twins in the nanoscale, complicates the crystalline structure more while more slip systems are usually operative near the grain boundary in the continuum scale.²⁴ Slip appears in the grain boundary of the nanowire under tensile loading, following the compressive loading.

By adding the maximum compression-induced strain and the maximum tension-induced strain, the maximum recoverable strain of the $\langle 100 \rangle / \{100\}$ copper nanowire is found to be approximately 21%.

B. Pseudoelasticity at 0 K and critical temperature

The twin region of the $\langle 100 \rangle / \{100\}$ nanowire, generated by compressive loading, is energetically stable, though it is deformed. This is because the $\{111\}$ surface, which is the side surface of the twin region, has a lower energy than the side surface of nanowire (the $\{100\}$ surface). The nanowire sustains deformed configuration through twinning, without any additional external loading. As the thermal energy cannot drive the $\{111\}$ surface to the $\{100\}$ surface, a lower-energy state to a high-energy state, the nanowire needs tensile loading to recover from the inelastic deformation. Based on this observation, a simulation at 0.1 K (0 K is an unrealistic temperature for simulation because temperature cannot be set to 0 K in *NVT* ensemble simulation) was performed. The other conditions for the simulation were the same as the ones at 300 K, i.e., the size of the copper nanowire, its orientation, the compressive strain (-0.1), and the organization of the cyclic loading.

The stress-strain curve of the copper nanowire at 0.1 K is shown in Fig. 8. During the cyclic loading, the stress-strain curve forms a hysteresis loop and the $\langle 100 \rangle / \{100\}$ copper nanowire shows pseudoelasticity even at 0.1 K. The investigations conducted by other researchers exhibit pseudoelasticity of the $\langle 110 \rangle / \{111\}$ nanowire above a critical temperature^{5,7} (about 200 K), the minimum temperature needed for pseudoelasticity. However, pseudoelasticity at 0.1 K shows that there is no critical temperature for the

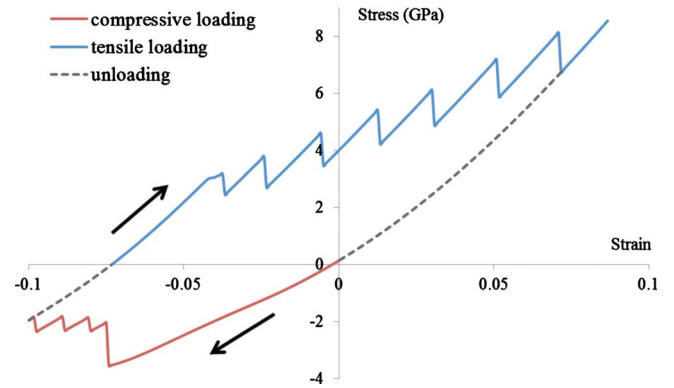


FIG. 8. (Color online) The stress-strain curve of the $\langle 100 \rangle / \{100\}$ Cu nanowire under cyclic loading at 0.1 K.

$\langle 100 \rangle / \{100\}$ nanowire. In contrast to typical macroscopic behavior of bulk SMAs, which exhibit pseudoelasticity at high temperatures (higher than the austenite finish temperature), and the $\langle 110 \rangle / \{111\}$ nanowire which exhibits pseudoelasticity at over a critical temperature, the result that the $\langle 100 \rangle / \{100\}$ copper nanowire does not require even a small amount of thermal energy for pseudoelasticity is remarkable.

The thermal energy is not a necessary condition for the pseudoelasticity of the $\langle 100 \rangle / \{100\}$ copper nanowire. However, it can influence on the pseudoelasticity of the nanowire which is already under an induced stress, as shown in Fig. 9. During cyclic loading, both nanowires, at 0.1 and 300 K, show pseudoelastic behavior, although the stress-strain curves take different paths at each temperature. The first difference in the behavior of both nanowires is the elastic modulus (slope of the curve) and the yield stress upon compressive loading. At the lower temperature (0.1 K), the nanowires are stiffer and have higher strength. During the subsequent tensile loading, there are similar differences in the yielding point and the elastic modulus. These differences, depending on the simulation temperature, result from the fact that the thermal energy supports the external strain loading energy to overcome SFE, the energy barrier. In other words, the thermal energy assists the external loading energy to generate deformation through twinning. Therefore, at the higher temperature (300 K), yielding occurs at lower stress levels,

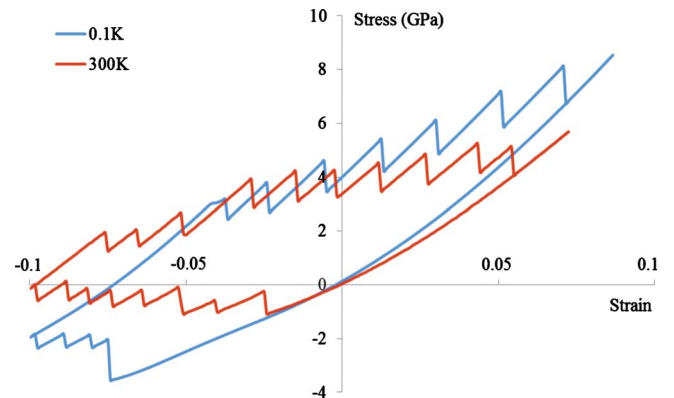


FIG. 9. (Color online) The stress-strain curves of the $\langle 100 \rangle / \{100\}$ Cu nanowires under cyclic loading at 0.1 and 300 K. Both nanowires are compressed to a strain of -0.1 .

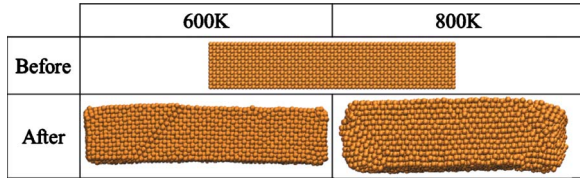


FIG. 10. (Color online) Snapshots of $\langle 100 \rangle / \langle 100 \rangle$ nanowires after the relaxation process at 600 and 800 K. The nanowire deformed by twinning during relaxation at 600 K. At 800 K, the nanowire is entirely reoriented to $\langle 110 \rangle / \langle 111 \rangle$.

under both compressive and tensile loading. Also the nanowire recovers its original orientation without twinning [in Fig. 2(b) F] at lower strains and stress levels.

C. Maximum allowable temperature

Only after stress is induced, temperature affects the behavior of the $\langle 100 \rangle / \langle 100 \rangle$ copper nanowire, as mentioned above. Although there is no critical temperature, the highest permissible temperature that exhibits and allows pseudoelasticity under cyclic loading exists.

The magnitude of the surface stress in the $\{100\}$ surface ranges from megapascal to gigapascal.^{26,27} This surface stress can drive reorientation only under external loading at lower temperatures. But, above 800 K, the $\langle 100 \rangle / \langle 100 \rangle$ copper nanowire is entirely reoriented to $\langle 110 \rangle / \langle 111 \rangle$ during the relaxation process without external loading, as shown in Fig. 10. Also, above 500 K, twinning occurs in the nanowire during relaxation. These twinning phenomena during relaxation are caused by the thermal energy, which helps the surface stress to overcome the SFE. The reorientation of other metal nanowires,^{5,7,27} caused by surface stress and thermal effect, have already reported.

Thermal energy can cause the reorientation of $\langle 100 \rangle / \langle 100 \rangle$ nanowire to $\langle 110 \rangle / \langle 111 \rangle$. This does not mean that temperatures can drive pseudoelasticity of the $\langle 100 \rangle / \langle 100 \rangle$ copper nanowire but high temperature acts as an obstacle to pseudoelasticity of the nanowire. Above 800 K, as the $\langle 100 \rangle / \langle 100 \rangle$ copper nanowire is entirely reoriented to

$\langle 110 \rangle / \langle 111 \rangle$ during the relaxation process, the nanowire shows pseudoelastic behavior, similar to that of the $\langle 110 \rangle / \langle 111 \rangle$ nanowire. Between 400 and 800 K, twinning appears on the $\langle 100 \rangle / \langle 100 \rangle$ nanowire during the relaxation process, and the atoms of the nanowire vibrate briskly because of the high temperature so, the nanowire shows unstable behavior under cyclic loading. Therefore, the maximum allowable temperature for stable pseudoelasticity of the $\langle 100 \rangle / \langle 100 \rangle$ copper nanowire, under cyclic loading, is about 400 K.

D. Continuous cyclic loading condition

The $\langle 100 \rangle / \langle 100 \rangle$ Cu nanowire maintains pseudoelastic behavior under continuous loading cycles, as shown in Fig. 11. In both 0.1 and 300 K cases, the nanowires exhibit pseudoelasticity during every cycle, and recover their initial perfect crystalline structures without any defects at the end of each cycle. As pseudoelastic behavior governed by twinning (nucleation, propagation, and annihilation of partial dislocations) at each cycle is an independent phenomenon, the stress-strain curves in Fig. 11 take slightly different paths during each loading cycle. But, all the unloading curves (after tensile loading) exactly overlap. Since the nanowires completely recover their original orientation (without any defect) under tensile loading, the nanowires which recover from the inelastic deformation behave in the elastic domain with residual stress. In other words, the nanowires are at an elastically stretched state after tensile loading ends (point F in Fig. 2) and recover their initial state (point A in Fig. 2) under the unloading process, via only one path.

If compression-induced strain over the maximum strain (12%) is applied on the $\langle 100 \rangle / \langle 100 \rangle$ copper nanowire, slips occur and are accumulated during the continuous cyclic loading. Since slip is a permanent plastic deformation, the nanowire does not exhibit pseudoelasticity after slip occurs. During the continuous cyclic loading, the nanowire does not recover its initial state, and the dislocations, including twinning and slip, pile up on the nanowire so, the stress-strain curve of the nanowire does not form a hysteresis loop, as shown in Fig. 12.

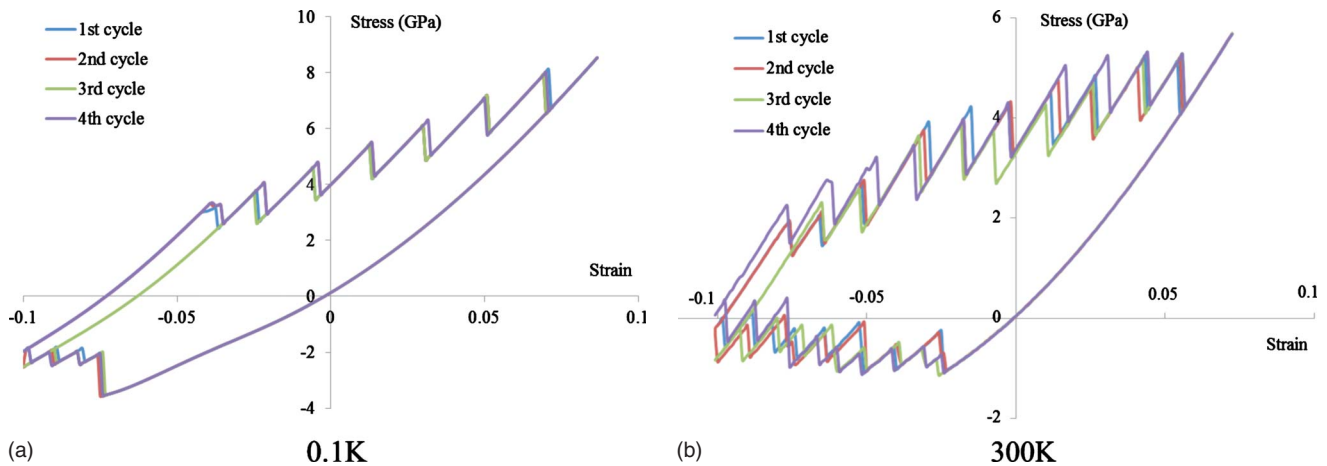


FIG. 11. (Color online) The stress-strain curves of the $\langle 100 \rangle / \langle 100 \rangle$ Cu nanowires under continued cyclic loading at (a) 0.1 K and (b) 300 K.

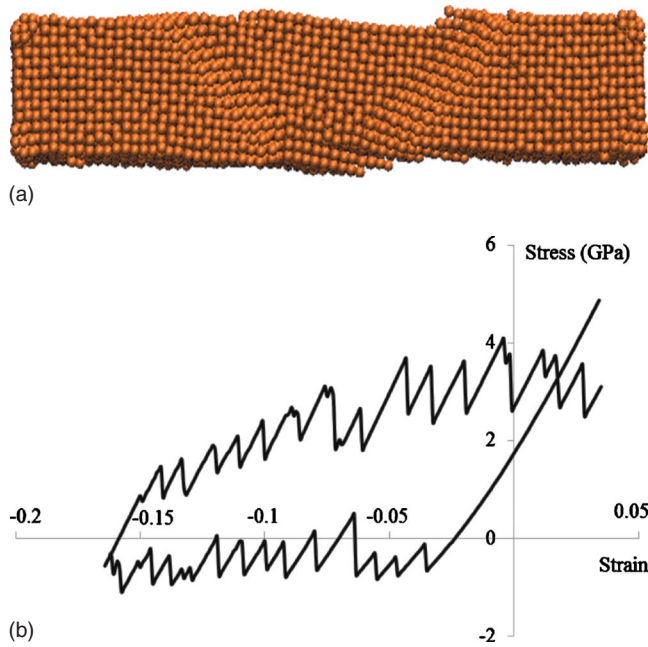


FIG. 12. (a) (Color online) Snapshot of the $\langle 100 \rangle / \{ 100 \}$ nanowire after the seventh cyclic loading and (b) the stress-strain curve of the nanowire during the seventh cyclic loading. The nanowire has a compressed strain of -0.17 at 300 K.

IV. CONCLUSION

The mechanical behavior of the $\langle 100 \rangle / \{ 100 \}$ nanowire was investigated by using MD simulations. Materials in the nanoscale have extraordinary properties which do not appear in the bulk. In the case of the $\langle 100 \rangle / \{ 100 \}$ copper nanowire, pseudoelasticity appears and is related to the deformation mechanisms and thermal energy. As the EAM potential is an approximation of many-atom interactions¹⁵ and it underestimates the surface energies,^{8,13} the energy value from MD simulations shows a low level of accuracy. But, the qualitative behavior of the nanowire analyzed using these simulations is valid because the EAM potential correctly predicts that the $\{ 110 \}$ surfaces have the highest energy, followed by the $\{ 100 \}$ and the $\{ 111 \}$ surfaces.⁸

The $\langle 100 \rangle / \{ 100 \}$ Cu nanowire exhibits pseudoelasticity under cyclic loading, which consists of compressive loading, unloading, tensile loading, and unloading. The maximum recoverable strain was about 22%, which is a remarkable amount compared with that of bulk SMAs. The pseudoelastic behavior originates from the reversibility of twinning. The deformation mechanism of the $\langle 100 \rangle / \{ 100 \}$ nanowire, upon compressive loading, is twinning. This causes the reorientation of the crystalline structure of the $\langle 100 \rangle / \{ 100 \}$ nanowire to $\langle 110 \rangle / \{ 111 \}$. Once reoriented, the $\langle 110 \rangle / \{ 111 \}$ region of the nanowire, under compressive loading, recovers to the initial crystalline structure, $\langle 100 \rangle / \{ 100 \}$, by twinning under tensile loading. As these two types of twinning cause different reorientations of the nanowire, their sequence establishes reversible twinning. The reversibility of twinning is fundamental to the pseudoelastic behavior of the $\langle 100 \rangle / \{ 100 \}$ copper nanowire.

The pseudoelasticity of the $\langle 100 \rangle / \{ 100 \}$ copper nanowire

is different from that of the $\langle 110 \rangle / \{ 111 \}$ nanowire because differences in their crystalline orientation results in different mechanical behaviors. First, the reorientation process by twinning depends on the crystalline orientation of the nanowire and the external loading condition. The $\langle 100 \rangle / \{ 100 \}$ copper nanowire is reoriented to $\langle 110 \rangle / \{ 111 \}$ by twinning deformation upon compressive loading while the $\langle 110 \rangle / \{ 111 \}$ nanowire is reoriented to $\langle 100 \rangle / \{ 100 \}$ by twinning upon tensile loading.⁸ Second, the stress-strain curves of the $\langle 100 \rangle / \{ 100 \}$ copper nanowire [Figs. 2(a), 8, and 11] show significant differences in the hysteresis shape and the ranges of stress and strain from those of $\langle 110 \rangle / \{ 111 \}$ copper nanowire [Fig. 3(b) in Ref. 3]. Also, the response behavior of these will never be similar during continuous cyclic loading. Third, the $\langle 100 \rangle / \{ 100 \}$ copper nanowire does not require a critical temperature to revert back to its original orientation but demands cyclic loading, including the tensile loading process, for pseudoelasticity. However, in the case of the $\langle 110 \rangle / \{ 111 \}$ nanowire, pseudoelasticity appears only over a critical temperature of 200 K. The difference between the existence and the nonexistence of the critical temperature is a crucial characteristic and a significant result in this investigation. This difference results from the energy gap between $\{ 111 \}$ and $\{ 100 \}$ surfaces. The thermal energy cannot drive the reorientation from the $\{ 111 \}$ surface, at lower-energy level, to $\{ 100 \}$, at higher-energy level.

At high temperatures, the thermal energy acts as a constraint in the pseudoelasticity of the $\langle 100 \rangle / \{ 100 \}$ nanowire. The thermal energy destabilizes the surfaces of the nanowire and drives twinning during the relaxation process. The maximum temperature for maintaining stable pseudoelastic behavior of the $\langle 100 \rangle / \{ 100 \}$ copper nanowire is about 400 K.

Pseudoelasticity of the $\langle 100 \rangle / \{ 100 \}$ copper nanowire is sustained by continuous cyclic loading below the maximum temperature because the nanowire reverts from the deformed state to its initial undeformed state with no defects at the end of each cycle.

Other metal nanowires with $\langle 100 \rangle / \{ 100 \}$ crystalline orientation are also expected to exhibit pseudoelasticity under similar conditions. Since all fcc nanowires have identical geometries, the SFEs of each metal alone would affect the deformation mechanism. Therefore, not all but, several fcc nanowires with $\langle 100 \rangle / \{ 100 \}$ orientation will show pseudoelasticity; for example, nickel is a strong candidate (the pseudoelasticity of Ni nanowire with $\langle 110 \rangle / \{ 111 \}$ orientation was reported in Refs. 5–7).

The pseudoelasticity of the $\langle 100 \rangle / \{ 100 \}$ copper nanowire allows for its use in various application fields. Since the nanowire is deformed under compressive loading, and it recovers its initial state upon tensile loading, the $\langle 100 \rangle / \{ 100 \}$ copper nanowire can be used as a cornerstone in nanodevices, sensors, and actuators. Moreover, if the sequence of the cyclic loading is guaranteed, it can be used in a wide range of applications because its pseudoelastic behavior can be started at any point on the hysteresis loop and, the $\langle 100 \rangle / \{ 100 \}$ copper nanowire can be used at various temperature ranges because it exhibits pseudoelasticity under

continuous cyclic loading, without requiring a critical temperature.

ACKNOWLEDGMENTS

This work was supported by National Research Founda-

tion of Korea through a National Research Laboratory program (Grant No. R0A-2009-000-20109-0) and World Class University program (Grant No. R31-2009-000-10083-0) funded by the Korean Ministry of Education, Science and Technology.

*Corresponding author. FAX: 82-02-886-1693; mhcho@snu.ac.kr

- ¹F. Milstein, J. Marschall, and H. E. Fang, *Phys. Rev. Lett.* **74**, 2977 (1995).
- ²H. Djohari, F. Milstein, and D. Maroudas, *Phys. Rev. B* **79**, 174109 (2009).
- ³W. Liang and M. Zhou, *Nano Lett.* **5**, 2039 (2005).
- ⁴W. Liang and M. Zhou, *ASME J. Eng. Mater. Technol.* **127**, 423 (2005).
- ⁵W. Liang and M. Zhou, *Phys. Rev. B* **73**, 115409 (2006).
- ⁶W. Liang and M. Zhou, *Philos. Mag.* **87**, 2191 (2007).
- ⁷H. S. Park, K. Gall, and J. A. Zimmerman, *Phys. Rev. Lett.* **95**, 255504 (2005).
- ⁸H. S. Park, K. Gall, and J. A. Zimmerman, *J. Mech. Phys. Solids* **54**, 1862 (2006).
- ⁹Y. Kondo and K. Takayanagi, *Phys. Rev. Lett.* **79**, 3455 (1997).
- ¹⁰V. Rodrigues, T. Fuhrer, and D. Ugarte, *Phys. Rev. Lett.* **85**, 4124 (2000).
- ¹¹V. Rodrigues and D. Ugarte, *Nanotechnology* **13**, 404 (2002).
- ¹²L. G. C. Rego, A. R. Rocha, V. Rodrigues, and D. Ugarte, *Phys. Rev. B* **67**, 045412 (2003).
- ¹³Y. Mishin, M. J. Mehl, D. A. Papaconstantopoulos, A. F. Voter, and J. D. Kress, *Phys. Rev. B* **63**, 224106 (2001).
- ¹⁴M. S. Daw and M. I. Baskes, *Phys. Rev. B* **29**, 6443 (1984).
- ¹⁵M. S. Daw, S. M. Foiles, and M. I. Baskes, *Mater. Sci. Rep.* **9**, 251 (1993).
- ¹⁶J. A. Zimmerman, H. Gao, and F. F. Abraham, *Modell. Simul. Mater. Sci. Eng.* **8**, 103 (2000).
- ¹⁷E. B. Tadmor and S. Hai, *J. Mech. Phys. Solids* **51**, 765 (2003).
- ¹⁸J. R. Rice, *J. Mech. Phys. Solids* **40**, 239 (1992).
- ¹⁹S. M. Foiles, M. I. Baskes, and M. S. Daw, *Phys. Rev. B* **33**, 7983 (1986).
- ²⁰W. Humphrey, A. Dalke, and K. Schulten, *J. Mol. Graphics* **14**, 33 (1996).
- ²¹W. G. Hoover, *Phys. Rev. A* **31**, 1695 (1985).
- ²²S. J. Plimpton, *J. Comput. Phys.* **117**, 1 (1995).
- ²³F. C. Frank, *Proc. Phys. Soc. London* **62A**, 202 (1949).
- ²⁴G. E. Dieter, *Mechanical Metallurgy* (McGraw-Hill, London, 1988).
- ²⁵M. Zhou, *Proc. R. Soc. London, Ser. A* **459**, 2347 (2003).
- ²⁶J. Diao, K. Gall, and M. L. Dunn, *Nano Lett.* **4**, 1863 (2004).
- ²⁷J. Diao, K. Gall, and M. L. Dunn, *Phys. Rev. B* **70**, 075413 (2004).
- ²⁸C. L. Kelchner, S. J. Plimpton, and J. C. Hamilton, *Phys. Rev. B* **58**, 11085 (1998).